

Accepted Manuscript

Synthesis and evaluation of dihydropyrimidinone-derived selenoesters as multi-targeted directed compounds against Alzheimer's disease

Flavio A.R. Barbosa, Rômulo F.S. Canto, Sumbal Saba, Jamal Rafique, Antonio L. Braga

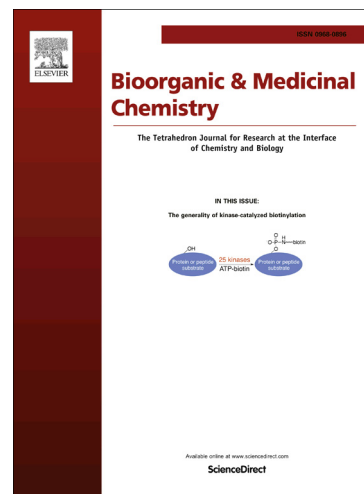
PII: S0968-0896(16)30718-0
DOI: <http://dx.doi.org/10.1016/j.bmc.2016.09.031>
Reference: BMC 13284

To appear in: *Bioorganic & Medicinal Chemistry*

Received Date: 29 July 2016
Revised Date: 9 September 2016
Accepted Date: 12 September 2016

Please cite this article as: Barbosa, F.A.R., Canto, R.F.S., Saba, S., Rafique, J., Braga, A.L., Synthesis and evaluation of dihydropyrimidinone-derived selenoesters as multi-targeted directed compounds against Alzheimer's disease, *Bioorganic & Medicinal Chemistry* (2016), doi: <http://dx.doi.org/10.1016/j.bmc.2016.09.031>

This is a PDF file of an unedited manuscript that has been accepted for publication. As a service to our customers we are providing this early version of the manuscript. The manuscript will undergo copyediting, typesetting, and review of the resulting proof before it is published in its final form. Please note that during the production process errors may be discovered which could affect the content, and all legal disclaimers that apply to the journal pertain.



Synthesis and evaluation of dihydropyrimidinone-derived selenoesters as multi-targeted directed compounds against Alzheimer's disease

Flavio A. R. Barbosa,^a Rômulo F. S. Canto,^a Sumbal Saba,^a Jamal Rafique^a and Antonio L. Braga^{a,*}

^a*Laboratório de Síntese de Substâncias Bioativas de Selênio, Centro de Ciências Físicas e Matemáticas, Departamento de Química, Universidade Federal de Santa Catarina, 88040-900, Florianópolis, SC-Brazil. <http://www.labselen.ufsc.br>*

* Corresponding author. Tel: +55 (48) 3721-6427;

e-mail address: braga.antonio@ufsc.br

Abbreviations: AD – Alzheimer's disease; ROS – reactive oxygen species; AChE – acetylcholinesterase; DHPMs – dihydropyrimidinones; GPx – glutathione peroxidase; TBARS - thiobarbituric acid reactive substances; NMR - nuclear magnetic resonance; IR – infrared spectroscopy; HMRS - high resolution mass spectrometry; APPI – atmosphere pressure photoionization; DPDS – diphenyl diselenide; BHT – butylated hydroxitoluene; MDA – malondialdehyde; M.P. – melting point.

Abstract

This paper describes the synthesis and evaluation of new dihydropyrimidinone(DHPM)-derived selenoesters as potential multi-targeted agents for the treatment of Alzheimer's disease. A series of DHPM-derived selenoesters were obtained with high structural diversity through a short and modular synthetic route. The antioxidant activity was evaluated by TBARS and iron chelation assays. These compounds were also evaluated as acetylcholinesterase inhibitors (AChEi). The compounds demonstrated good antioxidant activity, since they presented excellent lipid peroxidation

inhibition and good iron chelation activity. In addition, they showed acetylcholinesterase inhibition activity and some of them presented activity superior to that of the standard drug galantamine. The *in silico* predictions showed that the compound **1h** may present a good pharmacokinetic profile. Therefore, the series of DHPM-derived selenoesters described herein displayed good potential for the development of antioxidant and anticholinesterasic agents in the search for new multi-targeted therapeutics for the treatment of Alzheimer's disease.

Keywords: dihydropyrimidinones, selenoesters, antioxidant, Alzheimer's disease, selenium

1. Introduction

Alzheimer's disease (AD) is the most common neurodegenerative disease, affecting millions of people worldwide, and the prognosis is that this number will increase with population aging.¹ The disease is characterized by progressive memory loss and cognitive impairment, and it presents a complex pathophysiology, being described as a multifactorial disease.² Diverse factors such as amyloid- β deposits,³ decreased levels of acetylcholine,⁴ τ -protein aggregation⁵ and oxidative stress⁶ play significant roles in the progression of the disease.

Oxidative stress plays a pivotal role in the pathophysiology of AD, being one of the main causes of neuronal death.⁷ Reactive oxygen species (ROS) are overproduced in the brain of AD patients due to abnormal mitochondrial function that produces more O_2^- , which increases the concentration of H_2O_2 in the cytoplasm.⁸ The decreased concentrations of ferritin and increased free iron concentrations contribute to free radical generation through Fenton reactions.⁹ ROS damage membranes, proteins and DNA, as do lipid peroxidation

products, e.g. reactive aldehydes, which present much longer half-lives in the cell than the radicals, thus reacting with cell constituents leading to damage.¹⁰

Until now, the strategy of using single-targeted drugs has failed and the multi-targeted drug strategy is becoming a focus of research for the development of new drugs for the treatment of AD. The concept of multi-targeting is fully applicable to AD because of its multifactorial pathogenic mechanisms.¹¹ Nowadays, most of the palliative treatments available are drugs that inhibit acetylcholinesterase (AChE), based on the deficiency of acetylcholine in the central nervous system, e.g. tacrine,¹² galantamine,¹³ donepezil¹⁴ and rivastigmine,¹⁵ but their clinical usefulness is limited.¹⁶

Dihydropyrimidinones (DHPMs) are easily obtained *via* Biginelli multi-component reaction, and are reported as good antioxidants acting against lipid peroxidation and being effective as radical scavengers.¹⁷⁻¹⁹ Some analogs are better radical scavengers than resveratrol.²⁰ Also, this class of compounds presents AChE inhibitory activity,^{21,22} potent examples being reported with activities comparable to the standard drug galantamine.²³ Recently, we reported the synthesis and biological evaluation of a series of DHPMs functionalized with selenocyanides as potential multi-targeted therapeutics against AD.²⁴

Organoselenium compounds are very useful in synthetic transformations²⁵⁻²⁷ and also for biological purposes, since such compounds are well known antioxidants and glutathione peroxidase (GPx) mimetics,^{26,28-34} which is one of the most important natural antioxidant enzymes in the brain.³⁵ Very recently, Kumar and Engman showed that ebselenols are very good antioxidants, being more efficient than α -tocopherol for quenching peroxy radicals, and better GPx mimetics than ebselen.³⁶ Selenium might contribute in several ways against the progression of AD.³⁷ This element has been shown to modulate the cholinergic system and prevent oxidative damage in animal models of AD.³⁸

Diphenyl diselenide and its analogs, have also been studied in various animal models. These compounds can enhance the cognitive performance without inducing neurotoxicity,^{39,40} inhibit AChE activity, protect against β -amyloid induced neurotoxicity and improve the memory of mice,^{41–44} due to their antioxidant properties.

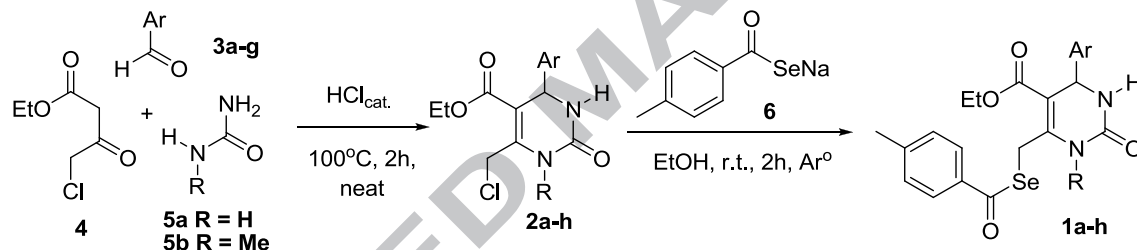
In this context, recent reports demonstrate the effective strategy of merging organoselenium compounds with known AChE inhibitors in the design of potential multi-targeted therapeutics for AD. Ebselen and donepezil were merged together in the same structure in order to develop potent human AChE inhibitors as well as good GPx mimics with the ability to penetrate the central nervous system with no acute toxicity.^{45,46} Also, some hybrids formed with tacrine and ebselen were also designed and they presented potent inhibitory activity against AChE and butyrylcholinesterase as well as being effective against hydrogen peroxide and peroxynitrite oxidants.⁴⁷ Recently, Wang and co-workers reported the synthesis and evaluation of clioquinol seleno-derivatives which demonstrated excellent antioxidant activities, inhibition of Cu(II)-induced amyloid- β aggregation and also good blood-brain barrier penetration *in vitro*.⁴⁸

As part of our wider research program aim at designing and developing biologically active new organoselenium compounds as well as eco-friendly processes,^{24,49–53} herein we report the design, synthesis and biological evaluation of a series of novel DHPM-derived selenoesters. The compounds were evaluated as antioxidants through the inhibition of lipid peroxidation in the thiobarbituric acid reactive species (TBARS) assay and also as iron chelating agents. The most active compounds were screened as inhibitors of the enzyme AChE, turning them into potential multi-targeted compounds for the treatment of Alzheimer's disease.

2. Results and Discussion

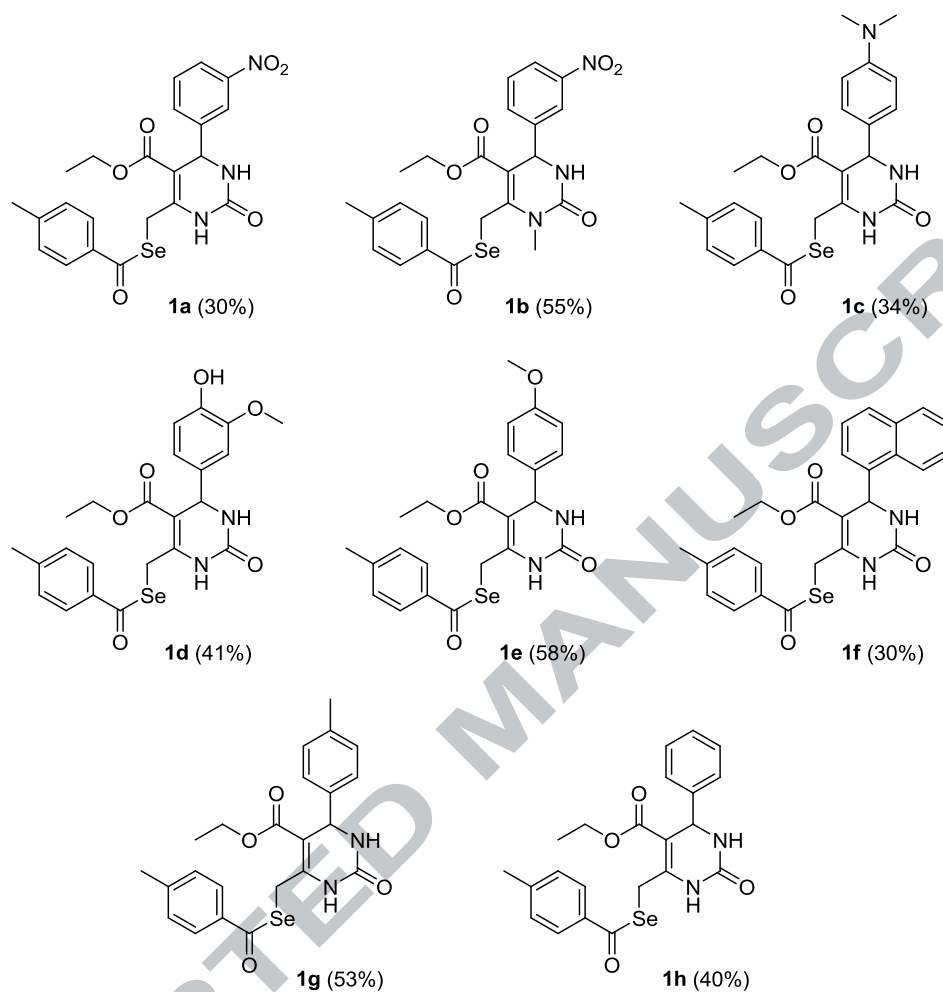
2.1. Chemistry and Biological evaluation

The synthesis of the DHPM-derived selenoesters **1a-h** was performed in a two-step pathway, affording the final compounds in moderate yields (Scheme 1). The intermediates 6-chloromethyl-DHPMs (**2a-h**) were synthesized in good yields from the three-component Biginelli reaction, using aromatic aldehydes (**3a-g**), ethyl 4-chloroacetoacetate (**4**) and urea (**5a**) or *N*-Me-urea (**5b**) at 100°C, under solvent-free conditions, catalyzed by HCl.²⁴ These 6-chloromethyl-DHPMs were reacted with the selenocarboxylate (**6**), generated *in situ* from the reaction of NaSeH with *p*-toluoyl chloride, at room temperature for 1 h, affording the target seleno-DHPM **1a-h** in 30-58% isolated yields.



Scheme 1. Synthesis of DHPM-derived selenoesters

A series of selenoesters functionalized with electron donating or withdrawing groups on the DHPM aromatic portion, as well as bicyclic aromatic structures were synthesized and the structures of the desired DHPM-derived selenoesters are shown in Figure 1. All compounds are stable at room temperature, even when exposed to light and an air atmosphere for prolonged times, and their analytical and spectroscopic data are in agreement with the expected structures.

Figure 1. Structures and yields of DHPM-derived selenoesters

In ^1H NMR spectra, the *N*-H resonance signals are usually registered as singlets in the ranges of *ca.* 5.51-8.14 ppm and 7.34-9.10 ppm. The aromatic protons of the DHPM nucleus appear at between 6.60 and 8.18 ppm and the two *doublets* of the aromatic moiety attached to the selenoester at 7.18 and 7.83 ppm. The proton of the carbon near to the NH appears as a *doublet* between 5.06 and 6.15 ppm. The two protons of the methylene that links the selenium to the DHPM core appear as an AB *quartet* at around 4.24 and 4.55 ppm. The characteristic *quartet* and *triplet* of the ethyl ester moiety appear at around 1.10 and 4.10 ppm, respectively. The ^{13}C NMR spectra show the characteristic carbonylic carbon of the selenoester moiety at around 195 ppm. In the HRMS (APPI), the molecular ion peaks M^+ presented the characteristic isotopic pattern of monoselenated compounds.

2.1.1 Inhibition of Thiobarbituric Acid Reactive Substances (TBARS) Production in Brain Homogenates

The synthesized seleno-DHPM **1a-h** were evaluated as antioxidants in the TBARS assay for lipid peroxidation. For the TBARS assay, the Ohkawa method was employed⁵⁴ and the iron-induced TBARS production in phospholipids was measured. These compounds were compared with the standard organoselenium antioxidants, ebselen and diphenyl diselenide (DPDS). The results for the comparative screening of compounds **1a-h** at a concentration of $100\mu\text{M}$ are shown in Figure 2 (Table S1 in the supporting information).

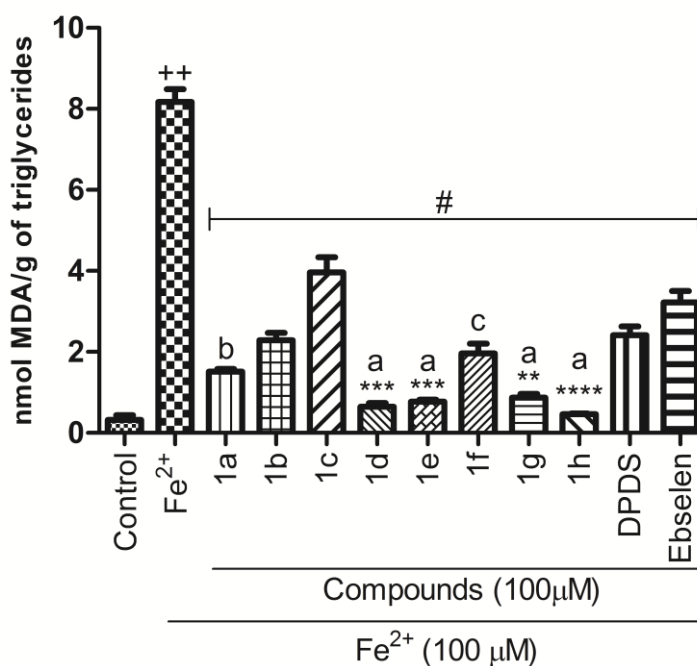
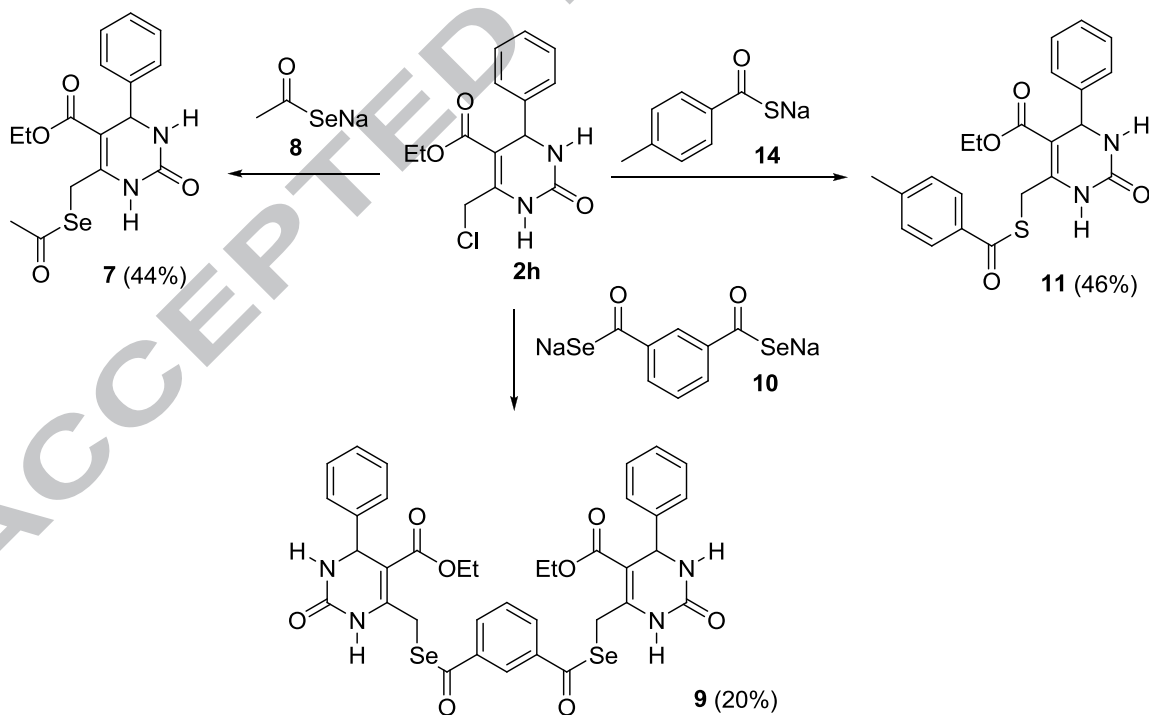


Figure 2. Effects of compounds **1a-h** on Fe²⁺ (100 µmol/L)-induced TBARS production in phospholipids extracted from egg yolk at 100µM (final concentration). Data are expressed as mean ± S.E.M of n= 3 independent experiments performed in duplicate. Data were analyzed by one-way analysis of variance (ANOVA), followed by Bonferroni's Multiple Comparison Test. ++*p* < 0.0001 vs control, #*p* < 0.0001 vs iron, ^a*p* < 0.0001 vs ebselen, ^b*p* < 0.001 vs ebselen, ^c*p* < 0.05 vs ebselen, *****p* < 0.0001 vs DPDS, ****p* < 0.001 vs DPDS, ***p* < 0.01 vs DPDS.

As can be seen in Figure 2, the DHPM-derived selenoesters **1a-h** inhibited iron-induced TBARS formation at 100µM as compared to the experiment without any of the compounds tested. Four of the tested compounds exhibited better activity than the standards ebselen and DPDS (**1d**, **1e**, **1g** and **1h**), whereas compounds **1a** and **1f** were only more active than ebselen. Compounds **1b** and **1c** did not show a significant difference when compared to the standards; however, both displayed good TBARS formation inhibition. The observed effects of different substituents in the aromatic ring on the activity do not adhere to a logical electronic effect, with a slightly more pronounced activity in the case of electron donating substituents. The presence of a methyl group in the place of hydrogen in the *N*-1 of the heterocycle seems to slightly reduce the activity, as can be seen on

comparing **1a** and **1b**. The most active compounds (**1d**, **1e**, **1g** and **1h**) were used in the concentration screening, which was carried out at concentrations of 100, 50, 25, 10, 5, and 1 μ M. The compounds displayed very good inhibition activity in a dose-dependent manner, being active even in low concentrations. For instance, **1h**, the most active compound, showed very good inhibition even at 10 μ M (graphs are available in SI).

In order to check the effect of the selenoester substitution pattern on the activity, we synthesized two new derivatives of the most active compound (**1h**) (Scheme 2). The acetyl substituted DHPM-derived selenoester **7** was synthesized from the reaction of 6-chloromethyl-DHPM **2h** with the selenocarboxylate **8** in 44% yield, and the dimeric selenoester **9** was prepared from the reaction of **2h** with bis-selenocarboxylate **10** in fair yield under the same conditions. We also synthesized the sulfur analog **11** in 46% yield, using the thiocarboxylate **14**, which was prepared using NaSH instead of NaSeH.



Scheme 2. Synthesis of **1h** analogues (**7**, **9** and **11**).

These compounds (**7**, **9**, **11**) and **1h** were compared in the TBARS assay with the ebselen and DPDS at 100 μM (Figure 3, Table S2 in the supporting information). These compounds inhibited TBARS formation when compared to the reaction with iron alone; however, only compound **1h** was more active than the standards. The effect of a modification in the selenoester structure was detrimental to the activity, as can be noted by comparing **7** and **9** to **1h**, discouraging further structural modifications in this position. The importance of the selenium atom with regard to the activity was also demonstrated through comparison of the activities of the selenoester **1h** and its less active sulfur analog **11**.

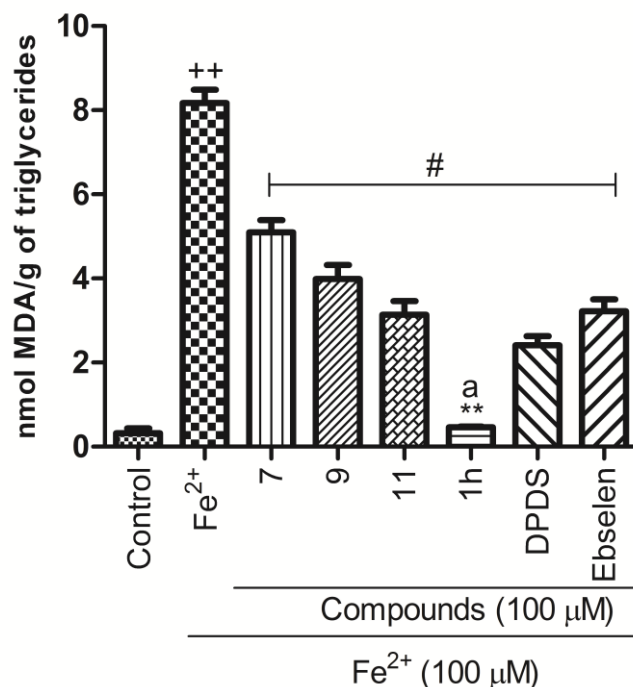


Figure 3. Effects of compounds **7**, **9**, **11** and **1h** on Fe²⁺ (100 $\mu\text{mol/L}$)-induced TBARS production in phospholipids extracted from egg yolk at 100 μM (final concentration). Data are expressed as mean \pm S.E.M of $n=3$ independent experiments performed in duplicate. Data were analyzed by one-way analysis of variance (ANOVA), followed by Bonferroni's Multiple Comparison Test. ++ $p < 0.0001$ vs control, # $p < 0.0001$ vs iron, ^a $p < 0.0001$ vs ebselen, ** $p < 0.01$ vs DPDS.

In order to investigate the effect of merging the selenoester moiety and the DHPM core in the same structure, we synthesized separate fragments of the hybrid, the selenoester **12** and the DHPM **13**, using the same reactions described above (see experimental section). The TBARS assay of these compounds showed that both separate fragments possess antioxidant activity, but the selenoester fragment **12** was more active. Nonetheless both fragments are less active than the hybrid of the two structures **1h**, indicating that both parts of the structure contribute to its overall antioxidant activity, and there may be a synergistic effect between the functional groups, enhancing the activity (Figure 4, (Table S3 in the supporting information)).

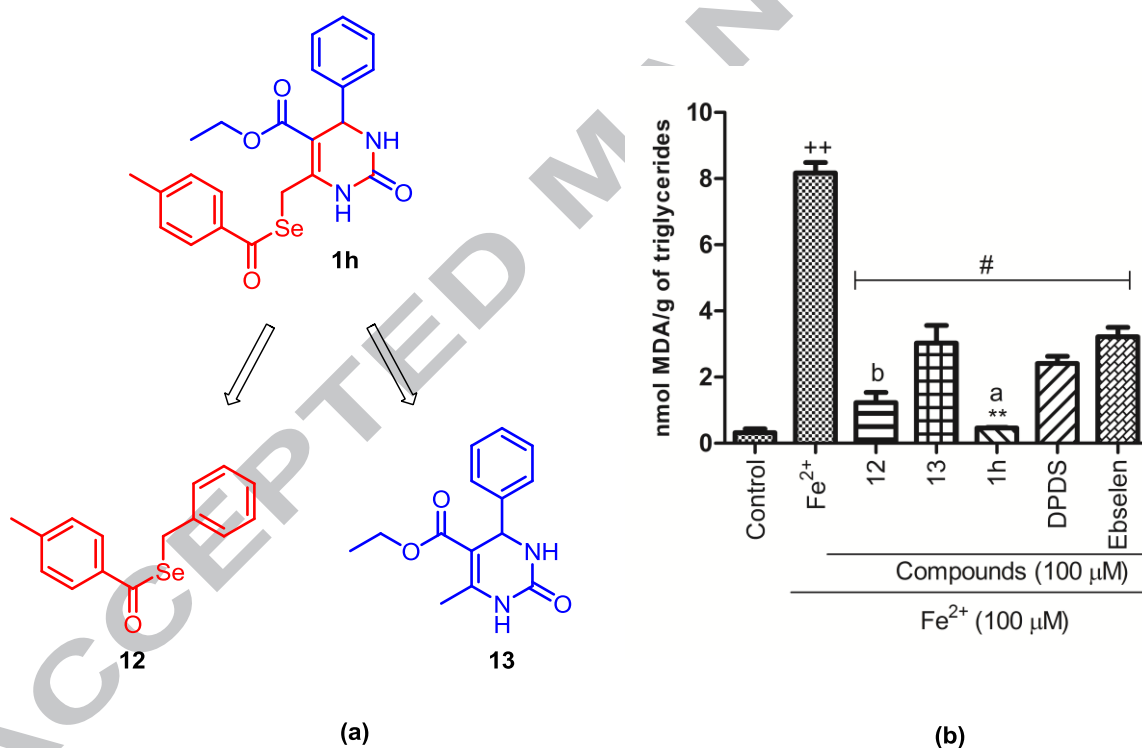


Figure 4. (a) Design of the fragments **12** and **13** from **1h**. (b) Effects of compounds on Fe²⁺ (100 μ mol/L)-induced TBARS production in phospholipids extracted from egg yolk at 100 μ M (final concentration). Data are expressed as mean \pm S.E.M of $n=3$ independent experiments performed in duplicate. Data were analyzed by one-way analysis of variance (ANOVA), followed by Bonferroni's Multiple Comparison Test. ++ $p < 0.0001$ vs control, # $p < 0.001$ vs iron, ^a $p < 0.001$ vs ebselen, ^b $p < 0.01$ vs ebselen, ** $p < 0.01$ vs DPDS.

2.1.2 Iron chelating activity

The synthesized compounds (**1a-h**, **7**, **9**, **11**, **12**, **13**) were evaluated as iron (II) chelators in the range of 5-100 μM applying the Minotti method⁵⁵ using BHT as the standard and the results are shown in Table 1. Of the DHPM-derived selenoesters **1a-h**, three presented EC_{50} values comparable to the standard BHT (compounds **1a**, **1e**, **1g**) and two presented values lower than the standard (**1d** and **1h**), **1d** being the most active compound, probably due to the substitution pattern (3-methoxy-4-hydroxy) in the aromatic ring, which is a well-known pattern in the antioxidant and chelation activity of phenolic compounds such as Apocynin, Vanillic acid and related compounds.^{56,57} The acyl selenoester (**7**) and dimer (**9**) analogs of compound **1h** presented lower iron chelation capacity than **1h**, indicating a detrimental effect on this activity with a variation in the selenoester side chain as well as in the TBARS assay. The bioisosteric replacement of selenium (**1h**) to sulfur (**11**) leads to a small decrease in activity, but compound **11** is still as active as the standard BHT. Both separate fragments of the hybrid **1h** (i.e., the selenoester **12** and the DHPM **13**) show activity comparable to that of BHT, but the EC_{50} values for **12** and **13** are higher than that for the hybrid **1h**, showing again that the hybridization contributes to greater activity.

Table 1. The EC₅₀ value of iron (II) chelation activity of compounds.

Compounds	Fe ²⁺ chelating activity ^a (EC ₅₀ μmol L ⁻¹)±SEM
1a	24.50±0.18
1b	32.83.±6.75
1c	29.6±1.74
1d	8.10±0.34*
1e	22.45±1.65
1f	35.50±1.46
1g	21.15±1.37
1h	10.45±1.55
7	41.16±2.60
9	29.85±5.09
11	20.2±3.81
12	22.35±0.81
13	15.85±2.05
BHT	23.30±0.36

^aThe compounds were tested in the range of 5-100 μM, Fe²⁺ 120 μM (final concentration). Results are expressed as Mean ± SEM of n = 3 independent experiments performed in duplicate. Data were analyzed by one-way analysis of variance (ANOVA), followed by Bonferroni's Multiple Comparison Test. **p* < 0.05 vs BHT.

2.1.3 Acetylcholinesterase inhibitory activity

The most active antioxidants and iron chelators (**1d** and **1h**) together with the **1h** analogues (**7**, **9** and **11**) and the fragments **12** and **13** were screened as inhibitors of AChE applying Ellmann's method,⁵⁸ using galanthamine as the standard, and the IC₅₀ results are shown in Table 2. The DHPM-derived selenoesters (**1d**, **1h**, **7** and **9**) showed good inhibitory activity against AChE, with compounds **1d**, **7** and **9** presenting activity comparable to the standard and compound **1h** being once again the most active compound. As in the case of the results for the TBARS assay and iron chelation activity, the inhibition of AChE was sensitive to modification of the selenoester side chain, leading to lower inhibition values (see compounds **7** and **9**). The bioisosteric replacement of selenium with sulfur also leads to a decrease in the activity and, although both fragments **12** and **13**

showed good inhibition values, they were still less active than the hybrid **1h**. These results indicate that the DHPM core contributes more to the interaction with the enzyme, but the hybridization of both fragments in the same structure produces a more active compound.

Table 2. The 50% inhibitory concentration (IC₅₀) of AChE of compounds.

Compounds	Acetylcholinesterase
	Inhibition ^a IC ₅₀ (μM)±SEM
1d	13.57±0.48
1h	7.21±0.48*
7	14.2±0.32
9	10.62±1.61
11	11.70±1.97
12	12.87±0.32
13	9.23±0.55
Galantamine	12.73±0.87

^aThe compounds were tested in the range of 5-50 μM. Results are expressed as mean ± SEM of n = 3 independent experiments performed in duplicate. Data were analyzed by one-way analysis of variance (ANOVA), followed by Tukey's multiple comparisons test. *Represents significant difference from galantamine at $p < 0.05$.

2.1.4 *In silico* prediction of pharmacokinetics properties

Furthermore, we performed an *in silico* prediction of the pharmacokinetics properties for compound **1h**. The open-source software Molinspiration⁵⁹ and OSIRIS Property Explorer⁶⁰ were used for calculations. Lipinski's rule of 5⁶¹ predicts that a potentially drug candidate will present a good pharmacokinetic profile if it meet some requirements, such as MW(Molecular Weight) ≤ 500, HBD(Hydrogen Bond Donors) ≤ 5, HBA(Hydrogen Bond Acceptors) ≤ 10 and Clog P ≤ 5.0 or MLogP ≤ 4.15. Veber and co-workers⁶² introduced other two important criteria for this type of analysis that is, to have 10 or fewer rotatable bonds and TPSA (Topological Polar Surface Area) ≤ 140 Å².

Compound **1h** satisfied both Lipinski and Veber criteria (Table 3) and the results showed that the compound may present good absorption and permeation after oral administration, turning it into a good drug candidate.

Table 3. *In silico* pharmacokinetics properties predictions for compound **1h**.

Property	Value
MLogP	4.56
CLogP	2.77
Molecular Weight	457.39
tPSA ^a (Å ²)	84.50
HBA ^b	6
HBD ^c	2
NRB ^d	8

^atPSA, Topological polar surface area; ^bHBA, H-bond acceptors; ^cHBD, H-bond donors; ^dNRB, Number of rotatable bonds.

3. Conclusions

In conclusion, we have synthesized a new series of DHPM-derived selenoesters and investigated their antioxidant activity in the TBARS assay, their capacity to chelate iron ions and also their inhibitory activity towards AChE. These hybrid compounds containing DHPM core and selenoester moiety presented superior activity profiles, as a result of synergistic effect from both fragments. The *in silico* predictions showed that the compound **1h** may present a good pharmacokinetic profile. Moreover, **1h** was the most promising compound of the series, emerging as a new lead for the development of multi-targeted compounds directed against alzheimer's disease.

4. Experimental Protocols

4.1. General Methods and Materials

NMR spectra (^1H NMR and ^{13}C NMR) were recorded on a Varian AS-400 or Bruker Avance 200 spectrometer. Chemical shifts (δ) are reported (in ppm) relative to the TMS (^1H NMR) and the solvent (^{13}C NMR). APPI-microTOF-Q II measurements were performed with a microTOF Q-II (Bruker Daltonics) mass spectrometer equipped with an automatic syringe pump (KD Scientific) for sample injection. The mass spectrometer was operated in the positive ion mode. The sample was injected using a constant flow ($3\mu\text{L}/\text{min}$). The solvent was a chloroform/methanol mixture. The APPI-microTOF-Q II instrument was calibrated in the mass range of 50–3000 m/z using an internal calibration standard (low concentration tuning mix solution) supplied by Agilent Technologies. Data were processed employing Bruker Compass Data Analysis software (version 4.0). Column chromatography was carried using Merck Silica Gel (230-400 mesh). Thin layer chromatography (TLC) was conducted using Merck Silica Gel GF₂₅₄ (0.25 mm thickness). For visualization, the TLC plates were either placed under ultraviolet light or stained with iodine vapor or acidic vanillin. The melting points were determined using a microscopy coverslip on a Micro Chemical MQA PF digital apparatus and are uncorrected. All common reagents and solvents were used as purchased unless otherwise noted.

4.2 Synthetic procedures

4.2.1. General procedure for the synthesis of compounds **2a-h** and **13**

The literature procedure was followed.²⁴ To a two-necked round-bottom flask, the appropriated aldehyde (10 mmol), ethyl 4-chloroacetoacetate or ethylacetoacetate (10 mmol), urea (1.2 g, 20 mmol) and 5 drops of concentrated HCl were added. The reaction mixture was stirred at 100 °C for the time required for the consumption of the starting materials, which was verified by TLC. After this time, the reaction mixture was poured into

crushed ice and water. The precipitate was filtered off and dried. The compounds were used without further purification.

Ethyl 6-(chloromethyl)-4-(3-nitrophenyl)-2-oxo-1,2,3,4-tetrahydropyrimidine-5-carboxylate (**2a**):

Yellow solid, M.P. 160 – 163 °C (Lit.⁶³ 162-164 °C), 80% Yield; ¹H NMR (200MHz, DMSO-d₆): δ = 1.11 (t, $J=7.3$ Hz, 3H); 4.04 (q, $J=6.8$ Hz, 2H); 4.62 (AB quartet, d, $J=10.7$ Hz, 1H); 4.78 (AB quartet, d, $J=10.7$ Hz, 1H); 5.37 (d, $J=3.4$ Hz, 1H); 7.62 – 7.73 (m, 2H); 8.02 (s, 1H); 8.12 – 8.16 (m, 2H); 9.69 (s, 1H); ¹³C NMR (50MHz, DMSO – d₆): δ = 14.2; 53.8; 60.6; 101.14; 121.5; 123.0; 130.8; 133.4; 146.5; 147.5; 148.3; 152.1; 164.4. HRMS (APPI) m/z calculated for C₁₄H₁₄ClN₃O₅ [M+H] 340.06947; found 340.06950.

Ethyl 6-(chloromethyl)-1-methyl-4-(3-nitrophenyl)-2-oxo-1,2,3,4-tetrahydropyrimidine-5-carboxylate (**2b**):

Light brown solid, M.P. 183 – 186°C, 82% Yield; ¹H NMR (200MHz, DMSO-d₆): δ (ppm) 1.16 (t, $J=7.0$ Hz, 3H); 3.24 (s, 3H); 4.12 (q, $J=7.0$ Hz, 2H); 5.03 (AB quartet, d, $J=11.6$ Hz, 1H); 5.20 (AB quartet, d, $J=12.1$ Hz, 1H); 5.37 (d, $J=4.0$ Hz, 1H); 7.68 – 7.74 (m, 2H); 8.12 – 8.18 (m, 2H); 8.31 (d, $J=3.5$ Hz, 1H); ¹³C NMR (100MHz, DMSO-d₆): δ = 18.6; 29.6; 51.9; 56.1; 65.3; 95.7; 121.5; 122.9; 130.3; 133.7; 144.4; 147.9; 151.1; 161.9; 169.95.

HRMS (APPI) m/z calculated for C₁₄H₁₆ClN₃O₅ [M+H] 354.0851; found 354.0857.

Ethyl 6-(chloromethyl)-4-(4-(dimethylamino)phenyl)-2-oxo-1,2,3,4-tetrahydropyrimidine-5-carboxylate (**2c**):

Yellow solid, M.P. 161 – 164°C, 30% Yield; ^1H NMR (200MHz, DMSO- d_6): δ = 1.13 (t, $J=7.1\text{Hz}$, 3H); 2.85 (s, 6H); 4.03 (q, $J=7.1\text{Hz}$, 2H); 4.60 (AB quartet, d, $J=10.5\text{Hz}$, 1H); 4.75 (AB quartet, d, $J=10.5\text{Hz}$, 1H); 5.08 (d, $J=3.2\text{Hz}$, 1H); 6.66 (d, $J=8.8\text{Hz}$, 2H); 7.06 (d, $J=8.7\text{Hz}$, 2H); 7.70 (bs, 1H); 9.38 (bs, 1H); ^{13}C NMR (50MHz, DMSO- d_6): δ = 13.9; 39.3; 40.2; 53.3; 59.8; 102.4; 112.3; 126.9; 145.2; 149.8; 152.2; 164.3. IR (KBr) (ν , cm^{-1}): 1615; 1638; 1689; 2811; 2929; 2978; 3127; 3233; 3363. HRMS (APPI) m/z calculated for $\text{C}_{16}\text{H}_{20}\text{ClN}_3\text{O}_3$ [M+H] 338.1266; found 338.1269.

Ethyl 6-(chloromethyl)-4-(4-hydroxy-3-methoxyphenyl)-2-oxo-1,2,3,4-tetrahydropyrimidine-5-carboxylate (**2d**):

Yellow solid, M.P. 163 – 165°C, 78% Yield; ^1H NMR (200MHz, DMSO- d_6): δ = 1.12 (t, $J=7.1\text{Hz}$, 3H); 3.72 (s, 3H); 4.04 (q, $J=7.2\text{Hz}$, 2H); 4.65 (AB quartet, d, $J=10.6\text{Hz}$, 1H); 4.72 (AB quartet, d, $J=10.6\text{Hz}$, 1H); 5.10 (d, $J=3.3\text{Hz}$, 1H); 6.61 – 6.81 (m, 4H); 7.75 (s, 1H); 9.42 (s, 1H); ^{13}C NMR (50MHz, DMSO- d_6): δ = 14.0; 53.7; 55.6; 60.0; 102.2; 110.8; 115.5; 118.6; 135.1; 145.7; 146.2; 147.5; 152.3; 164.4. IR (KBr) (ν , cm^{-1}): 1650; 1683; 2835; 2974; 3106; 3245; 3367; 3567. HRMS (APPI) m/z calculated for $\text{C}_{15}\text{H}_{17}\text{ClN}_2\text{O}_5$ [M+H] 341.0899; found 341.0898.

Ethyl 6-(chloromethyl)-4-(4-methoxyphenyl)-2-oxo-1,2,3,4-tetrahydropyrimidine-5-carboxylate (**2e**):

Yellow solid, M.P. 183 – 185°C (Lit.⁶⁴ 185- 186°C), 98% Yield; ^1H NMR (200MHz, DMSO- d_6): δ = 1.12 (t, $J=6.8\text{Hz}$, 3H); 3.72 (s, 3H); 4.04 (q, $J=7.3\text{Hz}$, 2H); 4.60 (AB quartet, d, $J=10.3\text{Hz}$, 1H); 4.77 (AB quartet, d, $J=10.8\text{Hz}$, 1H); 5.14 (d, $J=2.9\text{Hz}$, 1H); 6.89 (d, $J=8.8\text{Hz}$, 2H); 7.17 (d, $J=8.3\text{Hz}$, 2H); 7.78 (s, 1H); 9.45 (s, 1H); ^{13}C NMR (50MHz,

DMSO- d_6): δ = 13.9; 39.3; 53.4; 55.2; 60.1; 102.3; 113.9; 127.6; 136.2; 145.7; 152.2; 158.8; 164.4. HRMS (APPI) m/z calculated for $C_{15}H_{17}ClN_2O_4$ [M+H] 325.09496; found 325.09485.

Ethyl 6-(chloromethyl)-4-(naphthalen-1-yl)-2-oxo-1,2,3,4-tetrahydropyrimidine-5-carboxylate (**2f**):

Yellow solid, M.P. 132 – 135°C, 85% Yield; 1H NMR (200MHz, DMSO- d_6): δ = 0.82 (t, $J=7.1$ Hz, 3H); 3.77 – 3.94 (m, 2H); 4.75 (AB quartet, d, $J=10.5$ Hz, 1H); 4.86 (AB quartet, d, $J=10.6$ Hz, 1H); 6.13 (d, $J=3.1$ Hz, 1H); 7.45 – 7.64 (m, 4H); 7.84 – 7.97 (m, 3H); 8.30 – 8.34 (m, 1H); 9.58 (s, 1H); ^{13}C NMR (50MHz, DMSO- d_6): δ = 13.7; 39.4; 49.7; 59.9; 101.9; 123.7; 124.3; 125.7; 126.2; 128.3; 128.6; 130.0; 133.6; 139.7; 146.4; 151.7; 164.2. IR (KBr),(v, cm^{-1}): 1656; 1697; 2980; 3245. HRMS (APPI) m/z calculated for $C_{18}H_{17}ClN_3O_3$ [M+H] 345.1000; found 345.1004.

Ethyl 6-(chloromethyl)-2-oxo-4-*p*-tolyl-1,2,3,4-tetrahydropyrimidine-5-carboxylate (**2g**): Yellow solid, M.P. 165 – 168°C (Lit.⁶³ 164 - 166°C), 76% Yield; 1H NMR (200MHz, DMSO- d_6): δ = 1.17(t, $J=7.3$ Hz, 3H); 2.30(s, 3H); 4.09(q, $J=6.6$ Hz, 2H); 4.68 (AB quartet, d, $J=12.4$ Hz, 1H); 4.78 (AB quartet, d, $J=12.4$ Hz, 1H); 5.35 (d, $J=2.93$ Hz, 1H); 6.47 (s, 1H); 7.09 (d, $J=8.0$ Hz, 2H); 7.18 (d, $J=8.0$ Hz, 2H); 8.53 (s, 1H). ^{13}C NMR (50MHz, DMSO- d_6): δ = 13.9; 20.6; 53.6; 59.9; 102.0; 126.2; 129.0; 136.8; 141.0; 145.8; 152.1; 164.23. . HRMS (APPI) m/z calculated for $C_{15}H_{17}ClN_2O_3$ [M+H] 309.1000; found 309.0999.

Ethyl 6-(chloromethyl)-2-oxo-4-phenyl-1,2,3,4-tetrahydropyrimidine-5-carboxylate (**2h**):

Yellow solid, M.P. 173 – 175°C (Lit.⁶³ 174 - 176°C), 70% Yield; ¹H NMR (200MHz, DMSO-d₆): δ = 1.11 (t, *J*=7.1Hz, 3H); 4.04 (q, *J*=7.3Hz, 2H); 4.59 (AB quartet, d, *J*=10.6Hz, 1H); 4.78 (AB quartet, d, *J*=10.6Hz, 1H); 5.20 (d, *J*=3.3Hz, 1H); 7.24 – 7.37 (m, 5H); 7.85 (s, 1H); 9.49 (s, 1H); ¹³C NMR (50MHz, DMSO-d₆): δ = 13.8; 30.6; 53.9; 59.9; 101.8; 126.3; 127.5; 128.5; 143.9; 145.9; 152.0; 164.2. HRMS (APPI) *m/z* calculated for C₁₄H₁₅ClN₂O₃ [M+H] 295.0844; found 295.0847.

Ethyl 6-methyl-2-oxo-4-phenyl-1,2,3,4-tetrahydropyrimidine-5-carboxylate (**13**):

White solid, M.P. 211 – 214°C, 80% Yield; ¹H NMR (400MHz, DMSO-d₆): δ = 1.09 (t, *J*=6.6 Hz, 3H); 2.26 (s, 3H); 3.98 (q, *J*=7.0Hz, 2H); 5.16 (s, 1H); 7.24 – 7.34 (m, 5H); 7.77 (s, 1H); 9.23 (s, 1H). ¹³C NMR (100MHz, DMSO-d₆): δ = 14.13; 17.86; 54.06; 59.28; 99.35; 126.33; 127.34; 128.46; 144.92; 148.42; 152.28; 165.41.

4.2.2. General procedure for the synthesis of compounds **1a-h**, **7**, **9** and **12**

The literature procedure was followed.⁶⁵ To a two-necked round-bottom flask, under argon atmosphere, Se⁰ (0.395 g, 5.0 mmol) and ethanol (20 mL) were added followed by the portionwise addition of NaBH₄ (0.378 g, 10 mmol). The mixture was left under stirring until the solution became colorless. After this time, the appropriate acid chloride (5.0 mmol) was added dropwise and the reaction medium color immediately turned to yellow/orange. After 30 min, the electrophile (DHPM or benzyl bromide) (4.2 mmol) was added. The reaction was monitored by TLC until the total consumption of the electrophile. The reaction mixture was extracted with ethyl acetate/water and the organic phase dried over MgSO₄ and concentrated under vacuum and the crude product was purified by column chromatography (ethyl acetate:hexane).

Ethyl 6-((4-methylbenzoyl)selanyl)methyl-4-(3-nitrophenyl)-2-oxo-1,2,3,4-tetrahydropyrimidine-5-carboxylate (**1a**):

Slightly yellow solid, M.P. 169 – 173°C, 30% Yield; ^1H NMR (200MHz, CDCl_3): δ = 1.19 (t, $J=7.1\text{Hz}$, 3H); 2.41 (s, 3H); 4.11 (q, $J=7.2\text{Hz}$, 2H); 4.27 (AB quartet, d, $J=12.3\text{ Hz}$, 1H); 4.39 (AB quartet, d, $J=12.3\text{ Hz}$, 1H); 5.48 (d, $J=3.2\text{Hz}$, 1H); 7.01 (s, 1H); 7.26 (d, $J=8.2\text{ Hz}$, 2H); 7.43 (t, $J=7.9\text{Hz}$, 1H); 7.63 – 7.70(m, 2H); 7.79 (d, $J=8.2\text{ Hz}$, 2H); 8.03 – 8.09 (m, 1H); 8.16 (t, $J=1.9\text{ Hz}$, 1H); ^{13}C NMR (50MHz, CDCl_3): δ = 13.82; 21.53; 22.80; 54.29; 60.44; 99.90; 121.56; 122.56; 127.35; 129.41; 129.55; 132.67; 135.17; 145.34; 147.92; 149.48; 152.70; 164.62; 195.39. IR (KBr) (ν , cm^{-1}): 1603; 1634; 1644; 1693; 1713; 1937; 2868; 2935; 2947; 2978; 3114; 3196; 3239; 3310. HRMS (APPI) m/z calculated for $\text{C}_{22}\text{H}_{21}\text{N}_3\text{O}_6\text{Se}$ [M+H] 504.0670; found 504.0668.

Ethyl 1-methyl-6-((4-methylbenzoyl)selanyl)methyl-4-(3-nitrophenyl)-2-oxo-1,2,3,4-tetrahydropyrimidine-5-carboxylate (**1b**):

White solid, M.P. 63 – 65°C, 55% Yield; ^1H NMR (CDCl_3 , 200MHz): δ (ppm) 1.22 (t, $J=7.1\text{Hz}$, 3H); 2.41 (s, 3H); 3.29 (s, 3H); 4.16 (q, $J=7.1\text{Hz}$, 2H); 4.64 (bs, 2H); 5.50(d, $J=3.5\text{Hz}$, 1H); 7.27 (d, $J=8.3\text{Hz}$, 3H); 7.46 (t, $J=7.6\text{ Hz}$, 1H); 7.59 (d, $J=7.9\text{ Hz}$, 1H); 7.80 (d, $J=8.0\text{Hz}$, 1H); 8.07 – 8.15 (m, 2H); ^{13}C NMR (50MHz, CDCl_3): δ (ppm) 13.95; 21.59; 22.44; 29.94; 52.39; 60.73; 104.09; 121.48; 122.57; 127.26; 129.51; 129.56; 132.03; 135.39; 144.86; 145.17; 148.11; 150.82; 154.20; 164.96; 192.81. IR (KBr) (ν , cm^{-1}): 1685; 2880; 2925; 2955; 2980; 3090; 3235. HRMS (APPI) m/z calculated for $\text{C}_{23}\text{H}_{23}\text{N}_3\text{O}_6\text{Se}$ [M+H] 518.0826; found 518.0827.

Ethyl 4-(4-(dimethylamino)phenyl)-6-((4-methylbenzoyl)selanyl)methyl)-2-oxo-1,2,3,4-tetrahydropyrimidine-5-carboxylate (**1c**):

Yellow solid, M.P. 179 – 182°C, 34% Yield; ¹H NMR (200MHz, CDCl₃): δ = 1.20 (t, *J*=7.3Hz, 3H); 2.42 (s, 3H); 2.91 (s, 6H); 4.08 (q, *J*=7.1Hz, 2H); 4.27 (AB quartet, d, *J*=12.2Hz, 1H); 4.36 (AB quartet, d, *J*=12.2Hz, 1H); 5.27 (d, *J*=2.7Hz, 1H); 5.51 (bs, 1H); 6.63 (d, *J*=8.8Hz, 2H); 7.16 (d, *J*=8.8Hz, 2H); 7.27 (d, *J*=8.1Hz, 2H); 7.34 (bs, 1H); 7.81 (d, *J*=8.3Hz, 2H); ¹³C NMR (100MHz, CDCl₃): δ = 14.10; 21.79; 22.94; 40.45; 55.14; 60.26; 101.70; 112.36; 127.50; 127.66; 129.58; 131.41; 135.52; 145.45; 147.71; 150.19; 152.15; 165.44; 196.27. IR (KBr) (ν, cm⁻¹): 1615; 1630; 1687; 1713; 2809; 2923; 2980; 3110; 3227; 3369. HRMS (APPI) *m/z* calculated for C₂₄H₂₇N₃O₄Se [M+H] 502.1241; found 502.1241.

Ethyl 4-(4-hydroxy-3-methoxyphenyl)-6-((4-methylbenzoyl)selanyl)methyl)-2-oxo-1,2,3,4-tetrahydropyrimidine-5-carboxylate (**1d**):

White solid, M.P. 168 – 170°C, 41% Yield; ¹H NMR (200MHz, DMSO-d₆): δ = 1.10 (t, *J*=7.0Hz, 3H); 2.37 (s, 3H); 3.67 (s, 3H); 4.02 (q, *J*=7.0Hz, 2H); 4.27 (AB quartet, d, *J*=11.2Hz, 1H); 4.37 (AB quartet, d, *J*=11.0Hz, 1H); 5.07 (d, *J*=3.2 Hz, 1H); 6.61 – 6.71 (m, 2H); 6.79 (s, 1H); 7.37 (d, *J*=8.2Hz, 2H); 7.78 (d, *J*=8.2Hz, 3H); 8.95 (s, 1H); 9.09 (s, 1H); ¹³C NMR (50MHz, DMSO-d₆): δ = 14.06; 21.29; 23.81; 53.72; 55.52; 59.74; 100.87; 110.61; 115.32; 118.66; 127.01; 129.95; 135.37; 135.42; 145.23; 146.00; 147.42; 147.93; 152.08; 164.94; 193.35. IR (KBr) (ν, cm⁻¹): 1676; 1715; 2843; 2937; 2978; 3012; 3125; 3243; 3406. HRMS (APPI) *m/z* calculated for C₂₃H₂₄N₂O₆Se [M+H] 505.0874; found 505.0873.

Ethyl 4-(4-methoxyphenyl)-6-((4-methylbenzoyl)ethyl)-2-oxo-1,2,3,4-tetrahydropyrimidine-5-carboxylate (**1e**):

Slightly yellow solid, M.P. 169 – 170°C, 58% Yield; ¹H NMR (200MHz, CDCl₃): δ = 1.17 (t, *J*=7.8Hz, 3H); 2.41 (s, 3H); 3.75 (s, 3H); 4.08 (q, *J*=6.8Hz, 2H); 4.27 (AB quartet, d, *J*=11.7Hz, 1H); 4.36 (AB quartet, d, *J*=12.7Hz, 1H); 5.31 (d, *J*=2.9Hz, 1H); 6.20 (s, 1H), 6.79 (d, *J*=8.8Hz, 2H); 7.19 – 7.28 (m, 4H); 7.54 (s, 1H); 7.80 (d, *J*=7.8Hz, 2H); ¹³C NMR (50MHz, CDCl₃): δ = 13.99; 21.68; 22.93; 54.76; 55.08; 60.21; 101.41; 113.87; 127.55; 127.75; 129.50; 135.48; 135.82; 145.34; 148.02; 152.48; 159.07; 165.25; 195.84. IR (KBr) (ν, cm⁻¹): 1697; 2835; 2929; 2957; 3104; 3222; 3351. HRMS (APPI) *m/z* calculated for C₂₃H₂₄N₂O₅Se [M+H] 489.0924; found 489.0918.

Ethyl 6-((4-methylbenzoyl)ethyl)-4-(naphthalen-1-yl)-2-oxo-1,2,3,4-tetrahydropyrimidine-5-carboxylate (**1f**):

Slightly yellow solid, M.P. 174 – 177°C, 30% Yield; ¹H NMR (200MHz, CDCl₃): δ = 0.86 (t, *J*=7.1Hz, 3H); 2.43 (s, 3H); 3.84 – 4.01 (m, 2H); 4.31 (AB quartet, d, *J*=12.2Hz, 1H); 4.56 (AB quartet, d, *J*=12.2Hz, 1H); 5.57 (s, 1H); 6.26 (d, *J*=2.1Hz, 1H); 7.26 – 7.59 (m, 7H); 7.74 – 7.89 (m, 4H); 8.09(d, *J*=8.1Hz, 1H); ¹³C NMR (50MHz, CDCl₃): δ = 13.69; 21.70; 22.89; 50.79; 60.07; 100.27; 122.16; 124.50; 125.58; 126.51; 127.59; 128.46; 128.85; 129.55; 130.14; 133.85; 135.50; 138.38; 145.39; 149.05; 151.86; 165.21; 195.82. IR (KBr) (ν, cm⁻¹): 1640; 1695; 2853; 2925; 2955; 2976; 3110; 3233. HRMS (APPI) *m/z* calculated for C₂₆H₂₄N₂O₄Se [M+H] 509.0976; found 509.0975.

Ethyl 6-((4-methylbenzoyl)ethyl)-2-oxo-4-p-tolyl-1,2,3,4-tetrahydropyrimidine-5-carboxylate (**1g**):

Slightly yellow solid, M.P. 158 – 160°C, 53% Yield; ^1H NMR (200MHz, CDCl_3): δ = 1.18 (t, $J=7.1\text{Hz}$, 3H); 2.29 (s, 3H); 2.41 (s, 3H); 4.09 (q, $J=7.1\text{Hz}$, 2H); 4.29 (AB quartet, d, $J=12.4\text{Hz}$, 1H); 4.35 (AB quartet, d, $J=12.4\text{Hz}$, 1H); 5.33 (d, $J=2.9\text{Hz}$, 1H); 5.97 (s, 1H); 7.09 (d, $J=8.1\text{Hz}$, 2H); 7.19 (d, $J=8.1\text{Hz}$, 2H); 7.27 (d, $J=8.1\text{Hz}$, 2H); 7.47 (s, 1H); 7.81 (d, $J=8.2\text{Hz}$, 2H); ^{13}C NMR (50MHz, CDCl_3): δ = 13.99; 21.00; 21.70; 22.91; 55.06; 60.24; 101.30; 126.46; 127.57; 129.23; 129.51; 135.48; 137.47; 140.55; 145.35; 148.22; 152.50; 165.25; 195.90. IR (KBr) (ν , cm^{-1}): 1628; 1699; 2823; 2853; 2925; 2980; 3049; 3106; 3222; 3349. HRMS (APPI) m/z calculated for $\text{C}_{23}\text{H}_{24}\text{N}_2\text{O}_4\text{Se}$ [M+H] 473.0975; found 473.0979.

Ethyl 6-((4-methylbenzoyl)selanyl)methyl)-2-oxo-4-phenyl-1,2,3,4-tetrahydropyrimidine-5-carboxylate (**1h**):

Slightly yellow solid, M.P. 135 – 138°C, 40% Yield; ^1H NMR (200MHz, CDCl_3): δ = 1.15 (t, $J=6.8\text{Hz}$, 3H); 2.39 (s, 3H); 4.07 (q, $J=6.8\text{Hz}$, 2H); 4.29 (AB quartet, d, $J=12.8\text{Hz}$, 1H); 4.35 (AB quartet, d, $J=12.8\text{Hz}$, 1H); 5.35 (d, $J=2.9\text{Hz}$, 1H); 6.62 (s, 1H); 7.22 – 7.27 (m, 7H); 7.65 (s, 1H); 7.79 (d, $J=7.8\text{Hz}$, 2H); ^{13}C NMR (50MHz, CDCl_3): δ = 13.94; 21.68; 22.89; 55.30; 60.21; 101.07; 126.54; 127.54; 127.74; 128.54; 129.49; 135.46; 143.41; 145.32; 148.42; 152.46; 165.19; 195.80. IR (KBr) (ν , cm^{-1}): 1605; 1636; 1662; 1691; 1717; 1882; 1903; 1956; 1980; 2855; 2872; 2927; 2959; 2976; 3027; 3127; 3245. HRMS (APPI) m/z calculated for $\text{C}_{22}\text{H}_{22}\text{N}_2\text{O}_4\text{Se}$ [M+H] 459.0819; found 459.0822.

Ethyl 6-(acetyl)selanylmethyl)-2-oxo-4-phenyl-1,2,3,4-tetrahydropyrimidine-5-carboxylate (**7**):

Yellow solid, M.P. 156 – 158°C, 44% Yield; ^1H NMR (200MHz, CDCl_3): δ = 1.14 (t, $J=7.1\text{Hz}$, 3H); 2.47 (s, 3H); 4.05 (q, $J=7.1\text{Hz}$, 2H); 4.14 (s, 2H); 5.34 (d, $J=2.9\text{Hz}$, 1H); 6.28 (bs, 1H); 7.28 (s, 5H); 7.37 (bs, 1H); ^{13}C NMR (100MHz, CDCl_3): δ = 13.88; 23.58; 33.95; 55.09; 60.18; 101.12; 126.46; 127.71; 128.48; 143.33; 148.01; 152.63; 165.05; 199.76. IR (KBr) (ν , cm^{-1}): 1632; 1685; 2853; 2927; 2953; 2974; 3029; 3106; 3223; 3359. HRMS (APPI) m/z calculated for $\text{C}_{16}\text{H}_{18}\text{N}_2\text{O}_4\text{Se}$ [M+H] 383.0505; found 383.0507.

Phenyl-1,3-bis-ethyl-4-(phenyl)-6-((selenoformate)methyl)-2-oxo-1,2,3,4-tetrahydropyrimidine-5-carboxylate (**9**):

Yellow solid, M.P. 126 – 128°C, 20% Yield; ^1H NMR (200MHz, CDCl_3): δ = 1.18 (t, $J=7.1\text{Hz}$, 3H); 4.11 (q, $J=7.1\text{Hz}$, 2H); 4.38 (s, 2H); 5.40 (d, $J=2.0\text{Hz}$, 1H); 6.50 (bs, 1H); 7.25 – 7.29 (m, 6H); 7.58 (t, $J=8.0\text{Hz}$, 1H); 7.85 (bs, 1H); 8.10 (d, $J=6.5\text{Hz}$, 1H); 8.35 (bs, 1H). ^{13}C NMR (100MHz, CDCl_3): δ = 14.00; 23.84; 55.35; 60.41; 101.58; 126.11; 126.56; 127.91; 128.64; 129.72; 132.30; 138.68; 143.25; 147.70; 152.66; 165.14; 195.39. IR (KBr) (ν , cm^{-1}): 1638; 1695; 2906; 2933; 2978; 3031; 3088; 3237; 3351. HRMS (APPI) m/z calculated for $\text{C}_{36}\text{H}_{34}\text{N}_4\text{O}_8\text{Se}_2$ [M+H] 811.0788; found 811.0786.

Se-Benzyl 4-Methylbenzoselenoate (**12**):

Yellowish solid, M.P. 54 – 56°C, 85% Yield; ^1H NMR (400MHz, CDCl_3): δ = 2.35 (s, 3H); 4.31 (s, 2H); 7.20 (d, $J=7.8\text{Hz}$, 3H); 7.27 (t, $J=7.6\text{Hz}$, 2H); 7.35 (d, $J=7.4\text{Hz}$, 2H); 7.78 (d, $J=8.2\text{Hz}$, 2H). ^{13}C NMR (100MHz, CDCl_3): δ = 21.6; 28.8; 126.8; 127.3; 128.5; 128.9; 129.4; 136.2; 139.1; 144.6; 193.8.

4.2.3. General procedure for the synthesis of compound **11**

The literature procedure was followed for the synthesis of NaSH.⁶⁶ In a two-necked round-bottom flask, Na₂S·9H₂O (0.361 g, 1.5 mmol) and NaHCO₃ (0.126 g, 1.5 mmol) were solubilized in 10 ml of a mixture of ethanol-water (1:1). After 15 min, p-toluoyl chloride (0.198 ml, 1.5 mmol) was added. After 30 min, **2h** was added (0.294 g, 1.0 mmol). The consumption of 2h was monitored by TLC. The reaction mixture was extracted with ethyl acetate/water and the organic phase dried over MgSO₄ and concentrated under vacuum and the crude product was purified by column chromatography (ethyl acetate:hexane).

Ethyl 6-((4-methylbenzoylthio)methyl)-2-oxo-4-phenyl-1,2,3,4-tetrahydropyrimidine-5-carboxylate (**11**):

Slightly brown solid, M.P. 119 – 121 °C, 46% Yield; ¹H NMR (200MHz, CDCl₃): δ = 1.14 (t, J=7.2Hz, 3H); 2.39 (s, 3H); 4.07 (q, J=7.2Hz, 2H); 4.38 (s, 2H); 5.34 (d, J=2.9Hz, 1H); 6.74 (bs, 1H); 7.18 – 7.27 (m, 7H); 7.86 (m, 3H); ¹³C NMR (50MHz, CDCl₃): δ = 13.87; 21.57; 27.88; 55.20; 60.25; 101.94; 126.47; 127.51; 127.69; 128.48; 129.22; 133.34; 143.22; 144.87; 146.48; 152.53; 165.01; 192.44. IR (KBr) (ν, cm⁻¹): 1640; 1664; 1699; 1717; 2931; 2976; 3104; 3125; 3241; 3386. HRMS (APPI) m/z. calculated for C₂₂H₂₂N₂O₄S [M+H] 411.1373; found 411.1371.

4.4 Pharmacological evaluation

4.4.1. Thiobarbituric acid reactive substances (TBARS) assay

Production of thiobarbituric acid reactive species (TBARS) from phospholipid

The oxidative degradation of lipids by reactive oxygen species (ROS), called lipid peroxidation, results in the formation of highly reactive and unstable lipid peroxides.

Decomposition of lipid peroxides results in the formation of Thiobarbituric Acid Reactive Substances (TBARS), including malondialdehyde (MDA) which react with TBA (Thiobarbituric acid) resulting a pink coloured MDA-TBA adduct. Measuring TBARS levels offers a convenient method of determining the relative lipid peroxide content in a sample.

The production of TBARS from phospholipid was determined using the method of Ohkawa et al. (1979) with some modifications.⁵⁴ Thirty grams of egg yolk was mixed with isopropanol (90 mL), followed by the addition of water (90 mL). The mixture was stirred for 5 min and after filtration the liquid phase was centrifuged at 2000 x g to 10 min. The remaining supernatant was discarded and the white phase of the pellet was collected and re-suspended in 0.8 mL of water. The final concentration of triglycerides (1 mg/mL) was determined using an assay kit (Lab Test, MG, Brazil) according to the supplier's specifications.

The phospholipids derived from the yolk (0.05 mL) were incubated with and without freshly prepared iron sulfate (100 μ M) and with different concentrations of the organoselenium compounds (as show in the figures) together with potassium phosphate buffer (0.05 M, pH 7.5) and an appropriate volume of distilled water to give a total volume of 0.2 mL at 37°C for 1 h. The color reaction was carried out by adding 100 μ L of each acetic acid (pH 3.4) and 0.6% TBA, respectively. The reaction mixtures, including those diluted with 0.03 mM MDA standard, were incubated at 97°C for 1 h. The tubes were cooled and finally 0.58 mL of *n*-butanol was added followed by centrifugation at 1000 \times g. The organic layer (supernatant) was collected and absorbance was measured at 532 nm using the Cary 50 UV-Vis spectrophotometer. The TBARS unit was expressed as nmol of MDA/mg of triglycerides.

4.4.2. Iron chelation assay

The ability of compounds to chelate Fe^{2+} was determined using a modified version of the method of Minotti and Aust (1987) as described by Olabinri et al. (2010).^{55,67} In a tube, 268 μL of freshly prepared 120 μM FeSO_4 was added to a reaction mixture containing 336 μL of 0.1 M Tris-HCl (pH 7.4) and 200 μL of the test compounds at five different concentrations (5-100 μM ; prepared in methanol), followed by the addition of 436 μL of saline solution (0.9% NaCl, w/v). The reaction mixture was incubated for 10 min at 37°C before the addition of 260 μL of 1,10-phenanthroline (0.25%, w/v). The absorbance was subsequently measured at 510 nm using the Cary 50 UV-Vis spectrophotometer. Methanol was used instead of the sample solution as a control (A control) and BHT was used as a standard chelating agent.

Fe^{2+} chelating activity (%) was calculated by using the following formula:

$$\text{Fe}^{2+} \text{ chelating activity (\%)} = [(\text{Abs control} - \text{Abs sample}) / \text{Abs control}] \times 100$$

where Abs control is the absorbance of the control without the sample and Abs sample is the absorbance in the presence of the sample.

4.4.3. In Vitro Protocol of AChE inhibition

In the presence of the enzyme AChE, the compound ATCI (acetylthiocholine iodide) is hydrolyzed to produce acetate and thiocholine. The thiol (R-SH) group of thiocholine can react with the indicator compound DTNB (5-5'-dithio-bis-2-nitrobenzoic acid) to form TNB (5-thio-2-nitrobenzoate) and this reaction resulted in the development of a yellow color. The color intensity of the product is measured at 412 nm, and it is proportional to the enzyme activity. If an inhibitor, tested compounds, inhibits the enzyme,

then the rate of reaction will be slower and the optical density (absorbance) of the sample during the assay will be lower and hence no or less yellow color will be developed.

Acetylcholinesterase enzymatic activity was measured using the Ellman et al. (1961) method, with some modifications.⁵⁸ The assay medium (1 mL) consisted of deionized water, 0.1M phosphate buffer (pH 7.4), 0.01 M DTNB, the test compounds at five different concentrations dissolved in MeOH and an AChE (from electric eel) solution containing 0.8U mL⁻¹ and it was incubated for 15 min at 25°C. In the next step, 0.01 M acetylthiocholine iodide solution was added and the activity was determined by measuring the absorbance at 412 nm every 15 s for 5 or 10 min on a Cary 50 UV-Vis spectrophotometer at 25 °C. A control mixture containing methanol instead of the test samples was used. The absorbance value obtained was considered to be 100% activity. The percentage of AChE inhibitory activity (% IA) was calculated using the following equation:

$$I(\%) = 100 - (A \text{ sample}/A \text{ control}) \times 100$$

where “A sample” is the absorbance of the sample and “A control” is the absorbance without the sample. Plotting the inhibition percentage against the sample solution concentrations gave estimates of the IC₅₀ (concentration of the drug resulting in 50% inhibition of enzyme activity). Galantamine was used as the positive control.

Acknowledgements

The authors thank CEBIME, CNPq, INCT-Catálise, CAPES, TWAS and FAPESC for financial support.

References

1. Jellinger, K. A. *J. Neural Transm.* **2006**, *113*, 1603–1623.
2. Iqbal, K.; Grundke-Iqbal, I. *Neurobiol. Aging* **2000**, *21*, 901–902.
3. Castro, A.; Martinez, A. *Curr. Pharm. Des.* **2006**, *12*, 4377–4387.
4. Cummings, J. L. *Rev. Neurol. Dis.* **2004**, *1*, 60–9.
5. Alonso, A. del C.; Grundke-Iqbal, I.; Iqbal, K. *Nat. Med.* **1996**, *2*, 783–787.
6. Andersen, J. K. *Nat. Med.* **2004**, *10*, S18–25.
7. Butterfield, D. A.; Drake, J.; Pocernich, C.; Castegna, A. *Trends Mol. Med.* **2001**, *7*, 548–554.
8. Sutton, H. C.; Winterbourn, C. C. *Free Radic. Biol. Med.* **1989**, *6*, 53–60.
9. Petersen, R. B.; Nunomura, A.; Lee, H.; Casadesus, G.; Perry, G.; Smith, M. A.; Zhu, X. *Signal Transduction Cascades Associated with Oxidative Stress in Alzheimer's Disease*; **2007**; Vol. 11.
10. Bieschke, J.; Zhang, Q.; Powers, E. T.; Lerner, R. a.; Kelly, J. W. *Biochemistry* **2005**, *44*, 4977–4983.
11. León, R.; Garcia, A. G.; Marco-Contelles, J. *Med. Res. Rev.* **2013**, *33*, 139–189.
12. Kaufer, D. I.; Cummings, J. L.; Christine, D. *J. Geriatr. Psychiatry Neurol.* **1996**, *9*, 1–6.
13. Scott, L. J.; Goa, K. L. *Drugs* **2000**, *60*, 1095–122.
14. Bryson, H. M.; Benfield, P. *Drugs Aging* **1997**, *10*, 234–239.
15. Polinsky, R. J. *Clin. Ther.* *20*, 634–47.
16. Nordberg, A.; Svensson, A.-L. *Drug Saf.* **1998**, *19*, 465–480.
17. Prashantha Kumar, B. R.; Sankar, G.; Nasir Baig, R. B.; Chandrashekar, S. *Eur. J. Med. Chem.* **2009**, *44*, 4192–4198.
18. Vasconcelos, A. De; Oliveira, P. S.; Ritter, M.; Freitag, A.; Romano, L.; Quina, F.

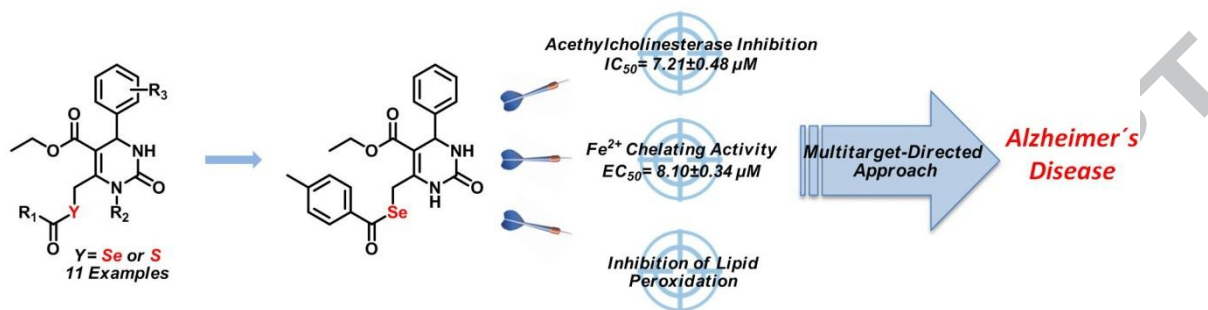
- H.; Pizzuti, L.; Pereira, C. M. P.; Francieli, M. J. *Biochem. Mol. Toxicol.* **2012**, *26*, 155–161.
19. Stefani, H. a; Oliveira, C. B.; Almeida, R. B.; Pereira, C. M. P.; Braga, R. C.; Cella, R.; Borges, V. C.; Savegnago, L.; Nogueira, C. W. *Eur. J. Med. Chem.* **2006**, *41*, 513–518.
20. Da Silva, D. L.; Reis, F. S.; Muniz, D. R.; Ruiz, A. L. T. G.; De Carvalho, J. E.; Sabino, A. a.; Modolo, L. V.; De Fátima, Â. *Bioorganic Med. Chem.* **2012**, *20*, 2645–2650.
21. Tomassoli, I.; Ismaili, L.; Pudlo, M.; de Los Ríos, C.; Soriano, E.; Colmena, I.; Gandía, L.; Rivas, L.; Samadi, A.; Marco-Contelles, J.; Refouvelet, B. *Eur. J. Med. Chem.* **2011**, *46*, 1–10.
22. Zhi, H.; Zhang, C.; Cheng, Z.; Jin, Z.; Huang, E.; Li, S.; Lin, H.; Wan, D. C.; Hu, C. *Med. Chem. (Los Angeles)*. **2013**, *9*, 703–709.
23. Arunkhamkaew, S.; Athipornchai, A.; Apiratikul, N.; Suksamrarn, A.; Ajavakom, V. *Bioorg. Med. Chem. Lett.* **2013**, *23*, 2880–2882.
24. Canto, R. F. S.; Barbosa, F. A. R.; Nascimento, V.; de Oliveira, A. S.; Brighente, I. M. C.; Braga, A. L. *Org. Biomol. Chem.* **2014**, *12*, 3470–3477.
25. Liotta, D.; Monahan III, R. *Science (80-.)*. **1986**, *231*, 356–361.
26. Bhabak, K. P.; Mugesh, G. *Acc. Chem. Res.* **2010**, *43*, 1408–1419.
27. Santoro, S.; Azeredo, J. B.; Nascimento, V.; Sancineto, L.; Braga, A. L.; Santi, C. *RSC Adv.* **2014**, *4*, 31521–31535.
28. McNeil, N. M. R.; Matz, M. C.; Back, T. G. *J. Org. Chem.* **2013**, *78*, 10369–10382.
29. Alberto, E. E.; Nascimento, V. Do; Braga, A. L. *J. Braz. Chem. Soc.* **2010**, *21*, 2032–2041.

30. Santi, C.; Tidei, C.; Scalera, C.; Piroddi, M.; Galli, F. *Curr. Chem. Biol.* **2013**, *7*, 25–36.
31. Kumakura, F.; Mishra, B.; Priyadarsini, K. I.; Iwaoka, M. *European J. Org. Chem.* **2010**, *2010*, 440–445.
32. Braga, A. L.; Rafique, J. In *PATAI'S Chemistry of Functional Groups*; **2013**; pp. 989–1052.
33. Nascimento, V.; Alberto, E. E.; Tondo, D. W.; Dambrowski, D.; Detty, M. R.; Nome, F.; Braga, A. L. *J. Am. Chem. Soc.* **2012**, *134*, 138–141.
34. Rafique, J.; Canto, R. F. S.; Saba, S.; Barbosa, F. A. R.; Braga, A. L. *Curr. Org. Chem.* **2015**, *20*, 166–188.
35. Klivenyi, P.; Andreassen, O. A.; Ferrante, R. J.; Dedeoglu, A.; Mueller, G.; Lancelot, E.; Bogdanov, M.; Andersen, J. K.; Jiang, D.; Beal, M. F. *J. Neurosci.* **2000**, *20*, 1–7.
36. Kumar, S.; Yan, J.; Poon, J.; Singh, V. P.; Lu, X.; Karlsson Ott, M.; Engman, L.; Kumar, S. *Angew. Chemie Int. Ed.* **2016**, *55*, 3729–3733.
37. Loef, M.; Schrauzer, G. N.; Walach, H. *J. Alzheimers. Dis.* **2011**, *26*, 81–104.
38. Souza, A. C. G.; Brüning, C. A.; Leite, M. R.; Zeni, G.; Nogueira, C. W. *Behav. Pharmacol.* **2010**, *21*, 556–562.
39. Rosa, R. M.; Flores, D. G.; Appelt, H. R.; Braga, A. L.; Henriques, J. A. P.; Roesler, R. *Neurosci. Lett.* **2003**, *341*, 217–20.
40. Stangherlin, E. C.; Luchese, C.; Pinton, S.; Rocha, J. B. T.; Nogueira, C. W. *Brain Res.* **2008**, *1201*, 106–113.
41. Pinton, S.; Brüning, C. a; Sartori Oliveira, C. E.; Prigol, M.; Nogueira, C. W. *J. Nutr. Biochem.* **2013**, *24*, 311–317.

42. Pinton, S.; da Rocha, J. T.; Zeni, G.; Nogueira, C. W. *Neurosci. Lett.* **2010**, *472*, 56–60.
43. Pinton, S.; Souza, A. C.; Sari, M. H. M.; Ramalho, R. M.; Rodrigues, C. M. P.; Nogueira, C. W. *Behav. Brain Res.* **2013**, *247*, 241–247.
44. Pinton, S.; da Rocha, J. T.; Gai, B. M.; Prigol, M.; da Rosa, L. V.; Nogueira, C. W. *Cell Biochem. Funct.* **2011**, *29*, 235–243.
45. Luo, Z.; Sheng, J.; Sun, Y.; Lu, C.; Yan, J.; Liu, A.; Luo, H. Bin; Huang, L.; Li, X. *J. Med. Chem.* **2013**, *56*, 9089–9099.
46. Luo, Z.; Liang, L.; Sheng, J.; Pang, Y.; Li, J.; Huang, L.; Li, X. *Bioorg. Med. Chem.* **2014**, *22*, 1355–1361.
47. Mao, F.; Chen, J.; Zhou, Q.; Luo, Z.; Huang, L.; Li, X. *Bioorganic Med. Chem. Lett.* **2013**, *23*, 6737–6742.
48. Wang, Z.; Wang, Y.; Li, W.; Mao, F.; Sun, Y.; Huang, L.; Li, X. *ACS Chem. Neurosci.* **2014**, *5*, 952–962.
49. Frizon, T. E.; Rafique, J.; Saba, S.; Bechtold, I. H.; Gallardo, H.; Braga, A. L. *European J. Org. Chem.* **2015**, *2015*, 3470–3476.
50. Rafique, J.; Saba, S.; Canto, R.; Frizon, T.; Hassan, W.; Waczuk, E.; Jan, M.; Back, D.; Da Rocha, J.; Braga, A. *Molecules* **2015**, *20*, 10095–10109.
51. Rafique, J.; Saba, S.; Rosário, A. R.; Zeni, G.; Braga, A. L. *RSC Adv.* **2014**, *4*, 51648–51652.
52. Saba, S.; Rafique, J.; Braga, A. L. *Catal. Sci. Technol.* **2016**, *6*, 3087–3098.
53. Saba, S.; Rafique, J.; Braga, A. L. *Adv. Synth. Catal.* **2015**, *357*, 1446–1452.
54. Ohkawa, H.; Ohishi, N.; Yagi, K. *Anal. Biochem.* **1979**, *95*, 351–358.
55. Minotti, G.; Aust, S. D. *Free Radic. Biol. Med.* **1987**, *3*, 379–387.

56. Heleno, S. a.; Martins, A.; Queiroz, M. J. R. P.; Ferreira, I. C. F. R. *Food Chem.* **2015**, *173*, 501–513.
57. Hatcher, C. H.; Singh, R. N.; Torti, F. M.; Torti, S. V. *Future Med. Chem.* **2009**, *1*, 1643–1670.
58. Ellman, G. L.; Courtney, K. D.; Andres, V.; Featherstone, R. M. *Biochem. Pharmacol.* **1961**, *7*, 88–95.
59. Molinspiration Cheminformatics, <http://www.molinspiration.com/cgi-bin/properties> (accessed July 2, 2016).
60. OSIRIS Property Explorer, <http://www.organic-chemistry.org/prog/peo/> (accessed June 1, 2014).
61. Lipinski, C.A.; Lombardo, F.; Dominy, B.W.; Feeney, P. J. *Adv. Drug Deliv. Rev.* **2001**, *46*, 3–26.
62. Veber, D. F.; Johnson, S. R.; Cheng, H.; Smith, B. R.; Ward, K. W.; Kopple, K. D. *J. Med. Chem.* **2002**, *45*, 2615–2623.
63. Sharghi, H.; Jokar, M. *Synth. Commun.* **2009**, *39*, 958–979.
64. Lebed', P. S.; Kos, P. O.; Polovinko, V. V.; Tolmachev, a. a.; Vovk, M. V. *Russ. J. Org. Chem.* **2009**, *45*, 921–927.
65. Athayde-filho, P. F. De; Souza, G. De; Morais, S. A. de; Botelho, J. R.; Barbosa-Filho, J. M.; Miller, J.; Lira, B. F. *ARKIVOC* **2004**, *2004*, 22–26.
66. Hodgson, H. H.; Ward, E. R. *J. Chem. Soc.* **1948**, *2*, 242.
67. Olabinri, B. M.; Eniyansoro, O. O.; Okoronkwo, C. O.; Olabinri, P. F.; Olaleye, M. T. *Int. J. Appl. Res. Nat. Prod.* **2010**, *3*, 13–18.

Graphical abstract



ACCEPTED MANUSCRIPT